Journal of the European Ceramic Society **16** (1996) 1221–1230
© 1996 Elsevier Science Limited
Printed in Great Britain. All rights reserved
PII:S0955-2219(96)00042-8
0955-2219/96/$15.00

Low-Temperature Sintering of Silicon Carbide with Li_2O–Al_2O_3–SiO_2 Melts as Sintering Aids

Y. Pan & J. L. Baptista

Departamento de Engenharia Cerâmica e do Vidro, Universidade de Aveiro, 3800 Aveiro, Portugal

(Received 13 December 1995; revised version received 5 January 1996; accepted 8 February 1996)

Abstract

With reference to sintering of SiC with Li_2O–Al_2O_3–SiO_2 (LAS) melts, equilibrium partial pressures of SiO, CO and Al_2O resulting from reactions of SiC and LAS have been thermodynamically estimated by taking carbon activity and temperature into account. Experimental work involving various LAS compositions and different powder beds showed that SiC/40 v% LAS (65·2 wt% SiO_2, 15·0 wt% Al_2O_3, 19·8 wt% Li_2O or 55·0 wt% SiO_2, 22·5 wt% Al_2O_3, 22·5 wt% Li_2O) can be densified in carbon rich powder bed to above 95%. The sintering temperature (100°C above m.p. of LAS) of these were the lowest of all. Thermodynamic estimations were used to explain the results. XRD, optical microscopy and SEM studies also supported the explanation. Copyright © 1996 Elsevier Science Ltd

1 Introduction

The difficulties with the sintering of silicon carbide ceramics have been attributed to the covalent nature of its chemical bond, particularly to the low surface energy and the low self diffusion coefficient resulting from the covalent bond. Successful sintering of silicon carbide has been reported and liquid-phase promotion or additives to improve diffusivity and surface energy were usually needed for the sintering. The most promising additives for liquid-phase sintering are metallic or oxide forms of aluminium,[1,2] mixtures of alumina and yttria,[3] and carbon and boron.[4] Aluminium or alumina, and alumina and yttria form a liquid phase during sintering of SiC. Carbon and boron were believed to improve the diffusivity of the components of SiC. Most of these sinterings had to be done on hot press and at high temperature (≥ 1900°C), which has, to some extent, limited the application of these technologies.

The Li_2O–Al_2O_3–SiO_2 (LAS) system has been successfully used as a binder of silicon carbide fibre and the composite made in this way had bending strength and fracture toughness as high as 1380 MPa and 17 MPa m^{-2}, respectively.[5] LAS has also been used as part of the matrix of a 55 wt% SiC–45 wt% (LAS/MAS/TiO_2) composite. The glass matrix was molten at the processing temperature playing a role of sintering aid of SiC.[6] Since liquid-phase-forming temperatures in the LAS system are relatively low, low-temperature liquid-phase sintering of silicon carbide with LAS melts as sintering aids could be a feasible method to widen the application of silicon carbide ceramics, for example, in cases where high-temperature strength is not important. Moreover, most LAS glasses can be crystallised through proper heat treatment, and therefore, the final parts could have satisfactory properties for some applications.

Reported in this paper is an exploration of liquid-phase sintering of SiC with LAS melts with eight different compositions. The first problem encountered was not the problem of the liquid-phase sintering on its own, but the problem caused by reactions of silicon carbide and LAS components. Systematic thermodynamic analysis of the reactions of silicon carbide with SiO_2, Li_2O and Al_2O_3 in LAS melts has been done and is here reported.

2 Chemical Equilibrium of SiC and LAS Melts

Chemical equilibrium of SiC and LAS melts involves the reactions of SiC with the SiO_2, the Li_2O and the Al_2O_3 in LAS glass. These reactions usually produce evaporating phases, such as SiO, Al_2O and CO, and solid phases, such as Li_2C_2 and Al_4C_3. Understanding and controlling these reactions is of great importance in liquid-phase sintering of SiC/LAS. Thermodynamic analyses of this system may start with the following reaction

$$SiC(s) + 2\,SiO_2(l) = 3\,SiO(g) + CO(g) \qquad (1)$$

At certain equilibrium temperature T and certain activity of SiO_2, A_{SiO_2} in LAS melts, the equilibrium partial pressures of SiO and CO, P_{SiO} and P_{CO} are related by

$$3 \ln P_{SiO} + \ln P_{CO} = f_1(T) + 2 \ln A_{SiO_2} \quad (2)$$

where $f_1(T) = \Delta_1 G^0/(-RT)$, $\Delta_1 G^0$ is the standard free energy change of reaction (1), R is the gas constant and T the absolute temperature.

The ranges of variation of P_{SiO} and P_{CO} are confined by possible reactions taking place as the carbon activity A_C and the silicon activity A_{Si} in silicon carbide are unity, respectively. For $A_C = 1$, a reaction taking place is:

$$C(s) + SiO_2(l) = CO(g) + SiO(g) \quad (3)$$

and

$$\ln P_{SiO} + \ln P_{CO} = f_3(T) + \ln A_{SiO_2} \quad (4)$$

For $A_{Si} = 1$, another reaction taking place is:

$$Si(l) + SiO_2(l) = 2\, SiO(g) \quad (5)$$

and

$$2 \ln P_{SiO} = f_5(T) + \ln A_{SiO_2} \quad (6)$$

In Fig. 1, in which P_{CO} and P_{SiO} are related by eqn (2) at different temperatures, the upper limits of P_{SiO} and P_{CO}, A, are determined by eqn (2) and eqn (4), and the lower limits, A', are determined by eqn (2) and eqn (6). Between the two limits, P_{SiO} and P_{CO} are determined by taking A_C or A_{Si} in eqn (3) and (5) into consideration. A_C and A_{Si} are not independent of one another, since the following equations will always be held at any temperature:

$$SiC(s) = Si(l) + C(s) \quad (7)$$

and

$$\ln A_{Si} + \ln A_C = f_7(T) \quad (8)$$

P_{SiO} as well as P_{CO} is thus a function of T and A_C.

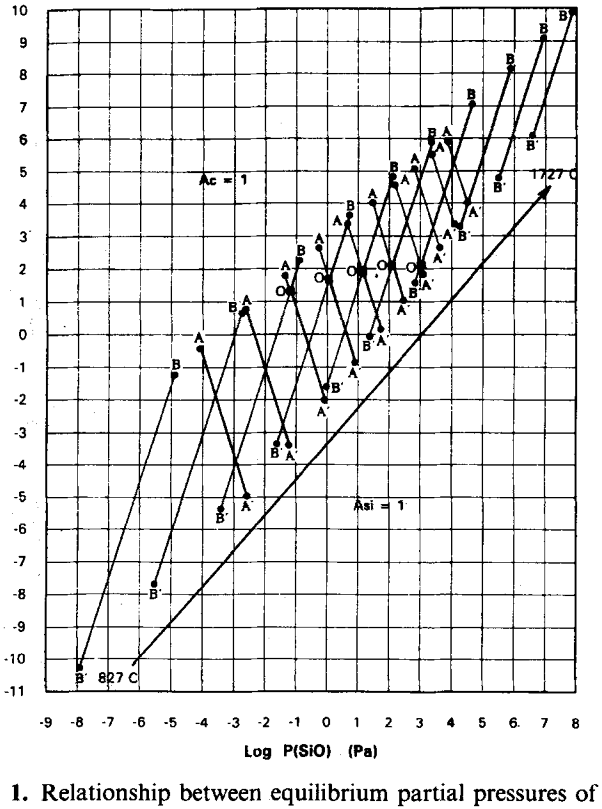

Fig. 1. Relationship between equilibrium partial pressures of CO and SiO in the reaction of SiC with LAS at different temperatures: AA' for reaction (1), BB' for reaction (9), O crossed points by AA' and BB' at temperatures 1027, 1127, 1227, 1327 and 1427°C. Bold lines refer to the predominant reactions at each temperature.

Another possible reaction taking place in the system SiC–LAS is the reaction of SiC with Li_2O, which may be expressed as follows:

$$3\, SiC(s) + 2\, Li_2O(s,l) + CO(g) = 3\, Li_2C_2(s) + 3\, SiO(g) \quad (9)$$

and

$$3 \ln P_{SiO} - \ln P_{CO} = f_9(T) + 2 \ln A_{Li_2O} \quad (10)$$

where A_{Li_2O} is the activity of Li_2O in LAS. Equation (10) is also shown in Fig. 1. The varying ranges of P_{SiO} and P_{CO} are also determined by the A_C in SiC. At $A_C = 1$, the upper limits of P_{SiO} and P_{CO}, B, in Fig. 1 are determined by eqn (10) and the following equations:

$$3\, C(s) + Li_2O(s,l) = Li_2C_2(s) + CO(g) \quad (11)$$

and

$$\ln P_{CO} = f_{11}(T) + \ln A_{Li_2O} \quad (12)$$

The lower limits B' are located by eqn (10) and the following:

$$2\, SiC(s) + Li_2O(s,l) = Li_2C_2(s) + SiO(g) + Si \quad (13)$$

and

$$\ln P_{SiO} = f_{13}(T) + \ln A_{Li_2O} \quad (14)$$

AA' has a negative slope of 3 and BB' has a positive slope of 3, which are determined by eqns (1) and (9) in double logarithm scale (Fig. 1).

$f_i(T) = \Delta_i G^0/(-RT)$ for each equation can be estimated by using thermodynamic data in JANAF Thermodynamical Tables.[7] As activities of SiO_2 and Li_2O are not considered, A-A' as well as B-B' at temperatures from 827°C (1100 K) to 1727°C (2000 K) have been estimated and the A-A' and B-B' in Fig. 1 are the results of these calculations.

In Fig. 1, it can be seen that, at 827°C (1100 K) and 927°C (1200 K), B-B' are on the left side of A-A', which means that the reaction between SiC and SiO_2 takes place, but the one between SiC and Li_2O will not, or that the interface between SiC and SiO_2 is not stable but the interface between SiC and Li_2O is. Above 1427°C (1700 K), B-B' are on the right side of A-A', which means that the interface between SiC and SiO_2 is stable and the interface between SiC and Li_2O is not. At 1027°C, 1127°C, 1227°C, 1327°C and 1427°C (1300, 1400, 1500, 1600 and 1700 K, respectively), *A-A'* and *B-B'* cross. The crossed points correspond to the following equilibrium

$$4\ \mathrm{SiC(s)} + 2\ \mathrm{SiO_2(s.l)} + 2\ \mathrm{Li_2O(s.l)} = 6\ \mathrm{SiO} + 2\ \mathrm{Li_2C_2} \quad (15)$$

in which A_C is fixed for each temperature (degree of freedom is reduced by one), and the P_{SiO} and P_{CO} at the crossed points, O, calculated accordingly.

Since Al_2O_3 is also an important component in LAS melts, the following equilibrium may also be established:

$$\mathrm{Al_2O_3(s)} + \mathrm{SiC(s)} = \mathrm{Al_2O(g)} + \mathrm{SiO(g)} + \mathrm{CO(g)} \quad (16)$$

and

$$\ln P_{Al_2O} + \ln P_{SiO} + \ln P_{CO} = f_{16}(T) \quad (17)$$

Therefore, P_{Al_2O} is also a function of T and A_C. Oxygen partial pressure can be also estimated, but it is very low ($\leq 10^{-19}$ Pa according to calculation) so that it is neglected hereafter.

P_{SiO}, P_{CO} and P_{Al_2O} as functions of T and A_C are plotted in Figs 2a, 2b and 2c, respectively. In these figures, A_C is varying from unity to $A_C = A_C(T)$ at which $A_{Si} = 1$ and T = 827, 927, ...1727°C. P_{SiO}, P_{CO} and P_{Al_2O} shown in Fig. 2 are those produced by thermodynamically most possible reactions. This means that, for T = 827°C and 927°C, they are produced by reaction (1), for T = 1527°C and above, they are produced by reaction (9), for T = 1027, 1127, 1227, 1327 and 1437°C, they are, in the carbon-rich side, produced by reaction (9) and in the silicon-rich side, produced by reaction (1). The inflections on these curves are corresponding to the alternatives chosen for the reactions. The partial pressures at these inflections are the same as the cross points O in Fig. 1.

The total pressure of evaporating phases, $P = P_{SiO} + P_{CO} + P_{Al_2O}$ is also plotted against A_C at different temperatures in Fig. 3. Besides the inflection resulting from P_{SiO} versus A_C, P_{CO} versus A_C and P_{Al_2O} versus A_C in Fig. 2, it can be also seen that the total pressures are above 10^5 Pa at temperatures above 1277°C as $A_C = 1$ or at temperatures above 1527°C as $A_{Si} = 1$. At each temperature, P is decreased with reducing A_C, but below 1527°C the minimum total pressure is not at $A_{Si} = 1$ and is somewhere in between but close to $A_{Si} = 1$. They may be picked up and are listed in Table 1.

In LAS melts the activities of SiO_2, Li_2O and Al_2O_3 are reduced. The reduced activities will affect the partial pressures of evaporating phases. But these effects are not taken into account because many factors affecting them are unknown. Thermodynamic and kinetics of reactions of SiC and Al_2O_3 and SiC and SiO_2 have been studied by Misra[8] and Jacobson *et al.*[9] but the sight angles were different from that of this paper. Some results can be translated to one another.

High total partial pressure is produced by consuming SiC and LAS melts, which, besides decomposing SiC, is harmful to the sintering process. Bloating bubbles filled with these high-pressure evaporating gases hinder shrinkage and leave large volume fractions of voids. Successful sintering has to be conducted in such conditions that the total partial pressure is as low as possible. According to Misra[8] and Jacobson, *et al.*,[9] the total pressure has to be lower than ambient in order to keep SiC stable.

3 Experimental

The starting materials used in this work are: α-SiC powder, produced by H. C. Starck, Germany, the BET specific surface of which is 5600 m²/kg and the carbon content of which is 28·8 wt%, lower than that of stoichiometric silicon carbide (29·2 wt%); lithium carbonate produced by M&B, England; silica precipitated and acid washed produced by BDH, England; and aluminium oxide also produced by BDH, England.

LAS glasses were prepared by making and firing the mixtures with various compositions shown in Table 2 in platinum crucibles. The amount of lithium carbonate in the mixture is 5 wt% higher than the designed composition so that the loss of lithium oxide during melting may be compensated. The firing temperature of each glass was about 200°C above the liquidus of the corresponding composition in the LAS phase diagram[10] and the dwell time at this temperature was more than one hour. The LAS melts were quenched into cold water to become transparent glasses, which were subsequently broken and milled by attrition milling into powders of sub-micron size. Some larger pieces of transparent glasses were chosen for the measurement of the 'theoretical' density of these glasses. Part of each glass was crystallised through heat treatment and the phases identified by XRD were all in agreement with the LAS phase diagram[10] being listed in Table 2. Eight different LAS systems listed in Table 2 were used as candidates of sintering aids of SiC ceramics.

Since this paper is focused on the effects of evaporating phases produced by the reaction of SiC and LAS melts on the sintering behaviour of SiC/LAS, the experimental work mainly covered the following:

α-SiC powder and each of the LAS glass powders listed in Table 2 were mixed and ball milled for 8 h in deionised water using an agate container and agate balls. The pH value of the suspension was adjusted in advance to 11 according to the suggestion of Almeida *et al.*[12] The good suspensions obtained were dried and powders were screened through 200 mesh. Samples with different LAS glasses were made exactly in the same way. The relative amount of LAS in all samples was the same, i.e. 40 v% which guaranteed enough liquid phase for rearrangement of silicon carbide particles during liquid-phase sintering. The samples were all first uniaxially pressed under 150 MPa and then cold isostatic pressed under 300 MPa into pellets of 10 mm diameter and 4–6 mm thickness. Sample number was the same number of the glass list in Table 2, for example, Sample 3 means SiC/40 v% glass 3. The

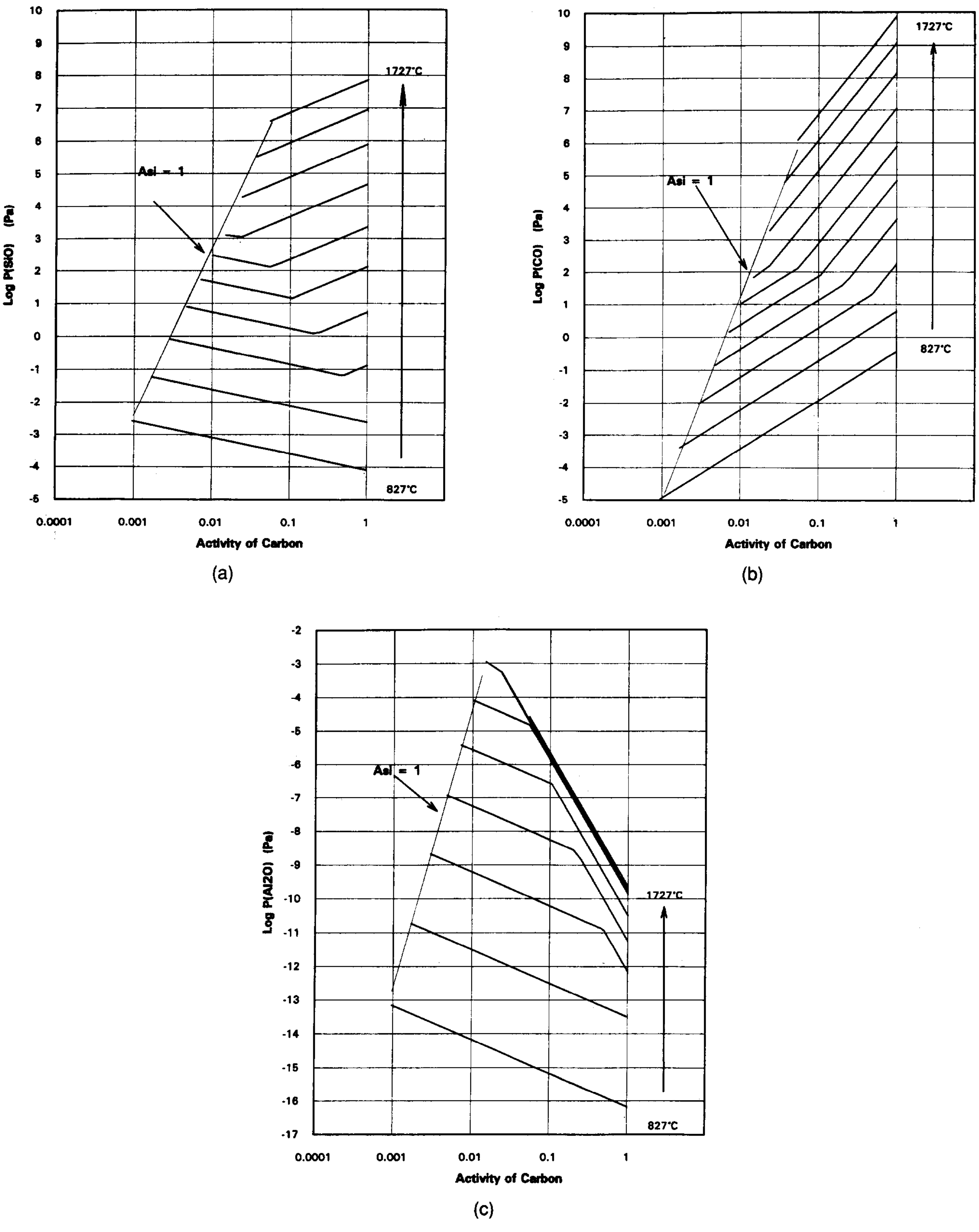

Fig. 2. (a) Carbon activity dependence of equilibrium partial pressure of SiO produced by predominant reactions at different temperatures. (b) Carbon activity dependence of equilibrium partial pressure of Al_2O produced by predominant reactions at different temperatures. (c) Carbon activity dependence of Al_2O produced by predominant reactions at different temperatures.

heating rate was 50°C/min, the sintering temperature was the temperature 100°C above the melting point (liquidus) of the glass in the sample and the dwell time was always 0·5 h. In cooling, the power supply to the sintering furnace was turned off and cooling water kept running. Three kinds of powder bed were chosen: PD1 was the same powder as the samples in which reaction of SiC with different components is assumed approximately stoichiometric, PD2 was an equimolar mixture of carbon black and each sample powder, in which carbon activity is unity, PD3 was an equimolar mixture of pure silicon and each sample powder, in which silicon activity is unity. Sintering processes were conducted in a furnace (Thermal Technology Inc., USA) with graphite heating element. Samples and powder beds were put in a closed alumina crucible so that they were isolated from the carbon atmosphere of the furnace. Inert gas (argon) was always used and the sintering process was always in a well-closed chamber, which means that argon was flowing through the furnace until 600°C and the furnace then tightly closed until the sintering was over, during which argon was over-pressured by 75 kPa. Weight, density and dimension of samples before and after sintering were carefully measured. XRD, SEM and optical microscopy were used for characterisations. Relative density and weight loss shown in this paper are the average of 12 samples of the same sort of composition in three runs in the same conditions.

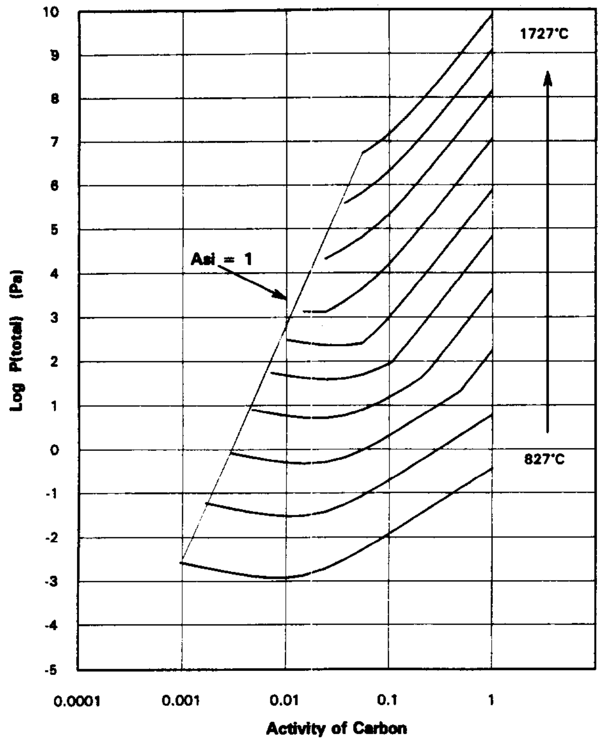

Fig. 3. Carbon activity dependence of total equilibrium partial pressure of evaporating phases produced by predominant reactions at different temperatures.

4 Results and Discussion

After several runs of closed-chamber sintering, some fine powder deposits on the furnace wall could

Table 1. Total partial pressure of evaporating phases in the equilibrium of SiC with LAS

Temp. (°C)	$P \times 10^5$ Pa as $A_C = 1$	$P_{min} \times 10^5$ Pa	A_C at P_{min}	$P \times 10^5$ Pa as $A_{Si} = 1$	A_C as $A_{Si} = 1$
827	3·70E-06	1·19E-08	0·010328	2·64E-08	0.000956
927	5·99E-05	3·02E-07	0·010328	5·99E-07	0·001665
1027	0·00176	4·74E-06	0·014716	8·33E-06	0·002919
1127	0·042209	5·03E-05	0·023875	7·93E-05	0·004723
1227	0·676196	0·000382	0·023875	0·000554	0·007168
1327	7·799071	0·00229	0·036792	0·003073	0·010328
1427	114·1237	0·012685	0·023875	0·013293	0·014716
1527	1409·583	—	—	0·205525	0·023875
1627	12054·54	—	—	3·819429	0·036792
1727	77309·13	—	—	51·075	0·054274

Table 2. LAS glasses used as SiC sintering aids in this paper

No	*Composition (wt%)* SiO_2	Al_2O_3	Li_2O	*Point in LAS phase diagram*[10]	*Liquidus* (°C)	*Melt at* (°C)	*Density* (g/cm³)
1	65·2	15·0	19·8	Eutectic of LS&(LA4S)	1027	1227	2·33
2	55·0	22·5	22·5	Triple point at 1050°C	1050	1257	2·23
3	64·8	21·5	13·7	Hyper-eutectic of LS*&LA4S	1250	1427	2·40
4	65·2	25·0	9·8	Hyper-eutectic of LS*&LA4S	1327	1527	2·46
5	47·6	40·5	11·9	$Li_2OAl_2O_32SiO_2$(LA2S)	1400	1607	2·50
6	64·5	27·4	8·1	$Li_2OAl_2O_34SiO_2$ (LA4S)	1425	1627	2·48
7	40·0	50·0	10·0	(LA2S + LA* + L5A* + Al_2O_3)[11]	1577	1777	2·80
8	10·0	77·8	12·2	Eutectic of $LiAl_2O_4$&Al_2O_3	1650	1877	2·81

Note: *LS = Li_2OSiO_2, LA = Li_2O Al_2O_3, L5A = $Li_2O5Al_2O_3$.

always be found and XRD analyses of these powders often gave Si, SiC and SiO_2, which are believed to be the products of low-temperature condensations of evaporating phases produced at high temperature by the reactions of SiC and LAS. This kind of reaction and the effects of these reactions on the sintering behaviour of SiC/LAS are the focal point of this paper.

Wettability of LAS glasses listed in Table 2 to SiC used in this study was proved by simply melting LAS on the top of SiC pellets. It has been found that all these glasses spread on the surface of SiC pellets and infiltrated into the pellets at the temperatures 100°C higher than the melting point, i.e. the sintering temperatures. The driving force of liquid-phase sintering is the capillary pressure between solid particles exerted by the liquid phase, which is dependent on the wettability of the liquid on the solid.[13] The resistance of liquid-phase sintering is from the viscosity of the liquid phase.[13] Since the sintering temperature was always 100°C higher than the LAS melting point, viscosity of these glasses should not be very different. Sintering time was kept to 30 min, which has been thought long enough for the completion of rearrangement of solid particles in LAS melts. It may be reasonably assumed that the controlling factor of the liquid-phase sintering of SiC in LAS is only the reactions of SiC with the components in LAS. These reactions consumed the materials within the samples and the evaporating phases produced permeated and filled voids inside the samples, strongly hindering centre-to-centre approaching and rearrangement of SiC particles in liquid phase. High partial pressure of the evaporating phases is apparently harmful to sintering.

Figures 4, 5 and 6 show the results (relative density and weight loss) of closed-chamber sintering of SiC with different LAS in PD1, PD2 and PD3, respectively. The numbers in these figures are the sample numbers. From these figures, it can be seen that, when the sintering temperature was

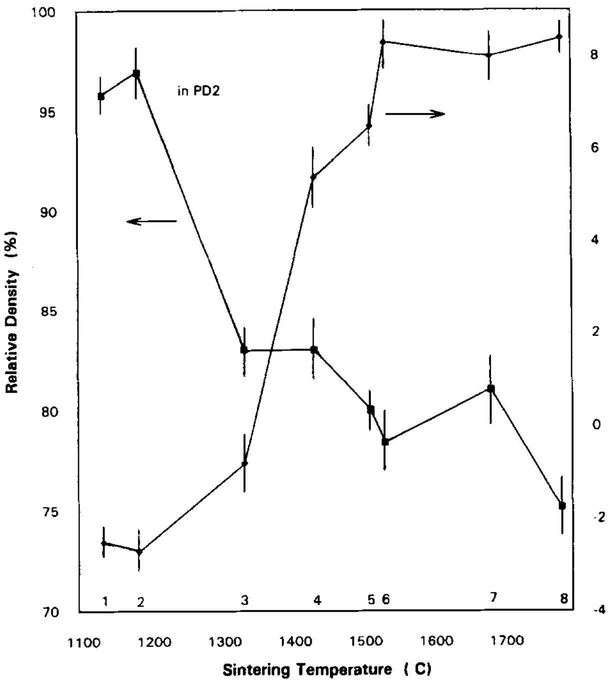

Fig. 5. Relative densities and weight losses of the samples in PD2 (carbon-rich). The numbers are sample number related to the sintering temperatures, 100°C higher than the liquidus (melting point) of LAS composition inside the samples.

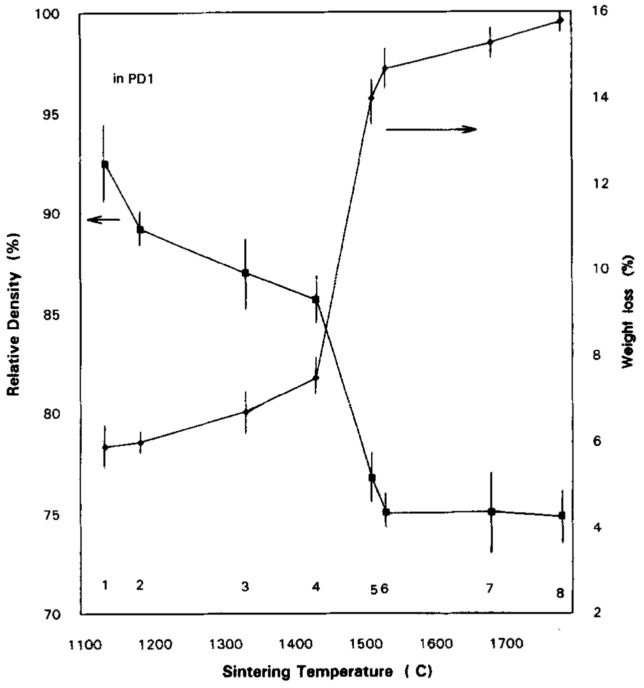

Fig. 4. Relative densities and weight losses of the samples in PD1 (stoichiometric). The numbers are sample number related to the sintering temperatures, 100°C higher than the liquidus (melting point) of LAS composition inside the samples.

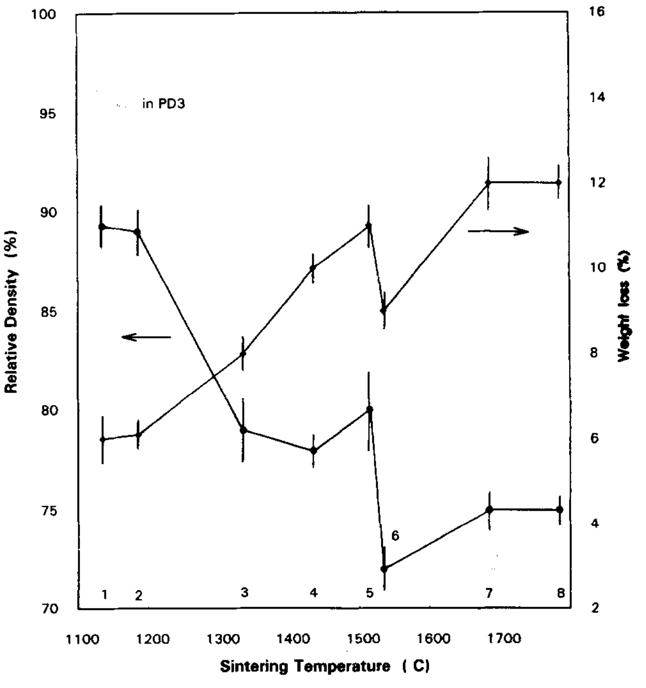

Fig. 6. Relative densities and weight losses of the samples in Pd3 (silicon-rich). The numbers are sample number related to the sintering temperatures, 100°C higher than the liquidus (melting point) of LAS inside the samples.

increased from sample 1 to 8, the relative density decreased. For samples sintered in PD1, the fastest relative density decrease appeared at temperatures from 1427°C (sample 4) to 1507°C (sample 5) (Fig. 4), and for samples sintered in PD2, density drop occurred from 1177°C (sample 2) to 1327°C (sample 3) (Fig. 5). This could be explained by the following:

In Fig. 4, since PD1 has the same composition of embedded samples, the reactions taking place in PD1 and inside samples should be thermodynamically the same. Higher relative density obtained at lower sintering temperature may be attributed to the lower partial pressures of evaporating phases resulting from these reactions taking place at these lower temperatures. It is suggested in Fig. 1 that, at any temperature from 1027 to 1427°C, *AA'* and *BB'* are crossed and a three-component reaction, reaction (15) may be dominant, particularly during the sintering at 1427°C (sample 4 in PD1). The total equilibrium partial pressure of evaporating phases produced by reaction (15) at 1427°C is relatively low (O in Fig. 1 and inflection points in Fig. 3) since the raw SiC powder used in this study was carbon-poor (28·8 wt% of carbon instead of 29·2 wt% for stoichiometric SiC). But at the temperatures above 1427°C, *BB'* is on the far right side of *AA'*, and reaction (9) is dominant. The total partial pressure of the evaporating phases is thus orders of magnitude higher than at temperatures of 1427°C and below (Fig. 3). The big jump of total equilibrium partial pressure from 1427 to 1507°C may be responsible for the fastest relative density decrease occurring in the same temperature range. The sudden increase in weight loss in Fig. 4 from 7·5% to 14% in the same range also supports this explanation. The sintered samples were X-rayed and Li_2C_2 was not found in sample 4 (PD1, 1427°C) and samples sintered below 1427°C, but was detected in sample 6 (PD1, 1527°C) (see A and C in Fig. 7). Li_2C_2 is the product of either reaction (9) or reaction (15). For low partial pressure (low temperature) samples, Li_2C_2 may be too small to be found. The Li_2C_2 detected in sample 6 (PD1 1527°C) was most likely produced by reaction (9) because only this reaction is predominant and gives higher pressure gas phases as well as a large amount of Li_2C_2.

In Fig. 5, sample 1 (PD2 1127°C) and sample 2 (PD2 1177°C) gave the highest relative densities and a negative weight loss (weight gain). A quick density decrease was found from sample 2 (PD2 1177°C) to sample 3 (PD2 1327°C) and the weight loss started to be positive after sample 2. As has been said, PD2 is carbon-rich, and therefore the highest total partial pressure of evaporating phases is expected (Figs 1 and 3). However, total equilibrium partial pressures of evaporating phases through reactions inside the samples are much lower because A_c inside the samples was reduced (SiC powder used was carbon-poor, 28·8% instead 29·2% for stoichiometric SiC; see also Fig. 3). Therefore, the reactions in PD2 prevailed over the possible reactions inside samples 1 and 2. Moreover, P_{SiO} and P_{CO} by PD2 (A_c = 1) at 1127°C and 1157°C may even make reaction (1) inside the samples proceed from right to left. No in-situ evaporating phases could be generated and no mass consumption could occur, and thus no sintering resistance existed. The weight gain found in these samples may also partially be caused by these. As sintering temperature was increased (from sample 3 PD2, 1327°C onwards), since the total partial pressures are above 0·1 MPa (Fig. 3), evaporating gases from PD2 may diffuse into the sample and tiny amount of carbon may be formed inside the samples through the reversible reaction (3), making A_c inside the samples change from less stoichoimetric towards 1 and initiating the reactions with high A_c between SiC and the LAS inside the samples. Partial pressure of evaporating gases higher than 0·1 MPa due to high carbon activity, may start to be created and high amount of mass consumption may occur, thus giving much lower relative density and positive weight loss (Fig. 5). This situation may be defined as an equilibrium between powder bed and sample.

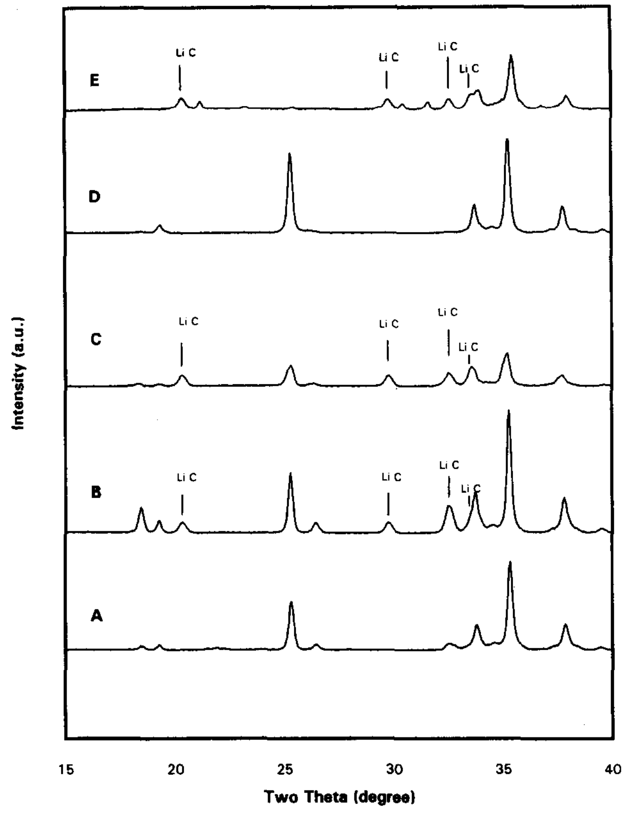

Fig. 7. X-ray diffraction results of sintered samples:

A:	Sample 4	PD1	1427°C	LiC not found
B:	Sample 3	PD2	1327°C	LiC found
C:	Sample 6	PD1	1527°C	LiC found
D:	Sample 1	PD2	1127°C	LiC not found
E:	Sample 7	PD3	1677°C	LiC found.

The establishment of this equilibrium certainly needs higher temperature and higher gas pressure. Sample 1 (PD2 1127°C) and sample 3 (PD2 1327°C) were also examined with XRD. Li_2C_2 was detected in sample 3 (see Fig. 7B), but not seen in sample 1 (see Fig. 7D). Li_2C_2 was also found in higher-temperature samples in PD2. This supports the presumption that gas-generating reactions really took place inside the sample 3 (PD2 1327°C) and other higher-temperature samples, but may not exist in low-temperature samples (e.g. sample 1 PD2 1127°C).

Weight gain found in samples 1 and 2 (PD2) could also possibly result from the condensation inside the samples of the evaporating phases generated by PD2 — mass transport from carbon-rich powder bed to sample during cooling. This condensation may also exist in other samples, and the weight loss in these samples was probably the net result of the condensation and gaseous phase evaporating (materials consuming). Samples 1 and 2 (PD2) in Fig. 5, which were 95·8% and 96·2% dense, respectively, were polished and photographs taken from optical microscopy are shown in Figs 8 A and B, respectively. They were also examined under SEM using back-scattering, shown in Fig. 9. They were basically close porosity. SiC particles were regularly arranged in the glass matrix (bright particles are SiC and dark background is glass). X-ray results (Fig. 7) show that the glass phase was crystallised even without post-sintering heat treatment.

Sample 7 (PD2 1677°C) was also examined under SEM (Fig. 10), β-SiC whiskers were found inside a hole of this sample. SiC whiskers are usually formed through gas reaction which has been discussed by many researchers, typically referred to Miller.[14] The appearance of SiC whiskers provides more evidence that evaporating phases were generated during sintering and the evaporating phases could be condensed to become secondary carbide, e.g. SiC whiskers. SEM observation was also done on sample 4 (PD2 1427°C); small particle agglomerates between SiC grains shown in Fig. 11 could

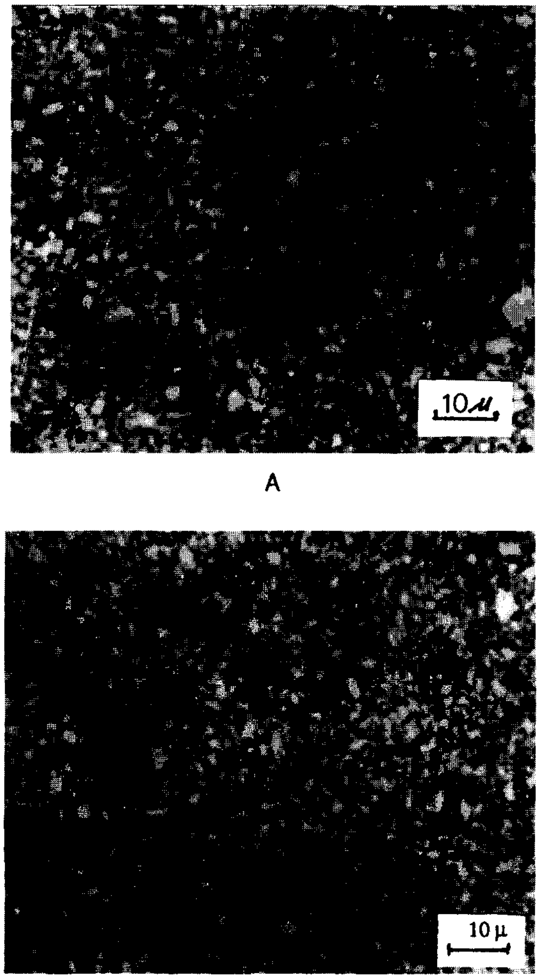

Fig. 8. Optical micrographs of polished samples
A: Sample 1 PD2 1127°C
B: Sample 2 PD2 1177°C.

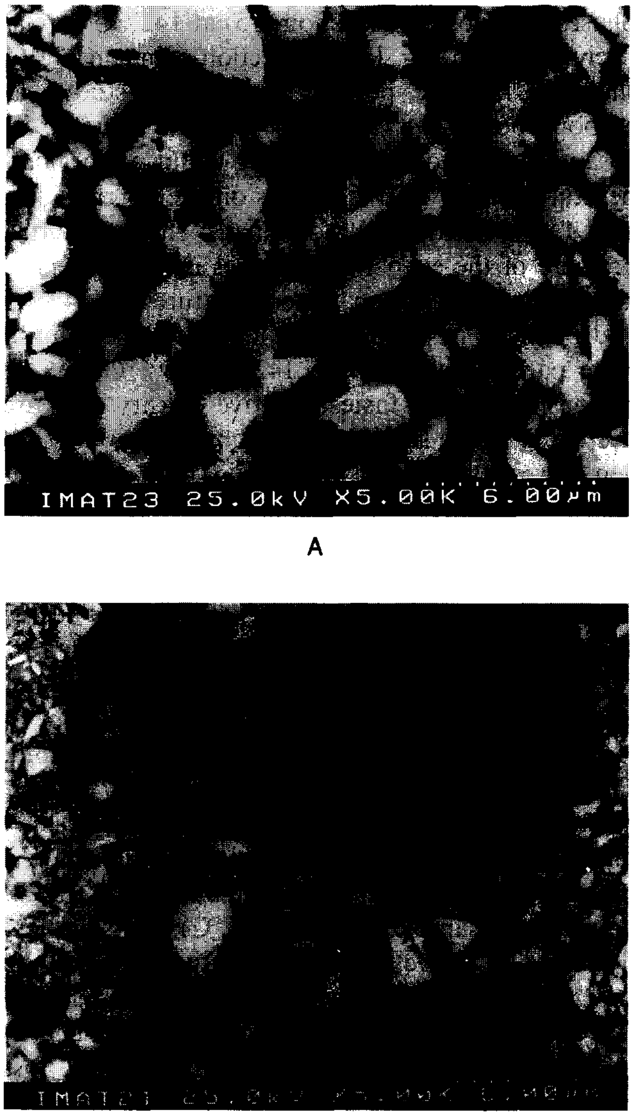

Fig. 9. SEM back-scattering micrographs of polished samples
A: Sample 1 PD2 1127°C
B: Sample 2 PD2 1177°C.

Fig. 10. SEM secondary electron micrographs of sample 7 sintered in PD2 at 1677°C. (SiC whiskers were found in a hole).

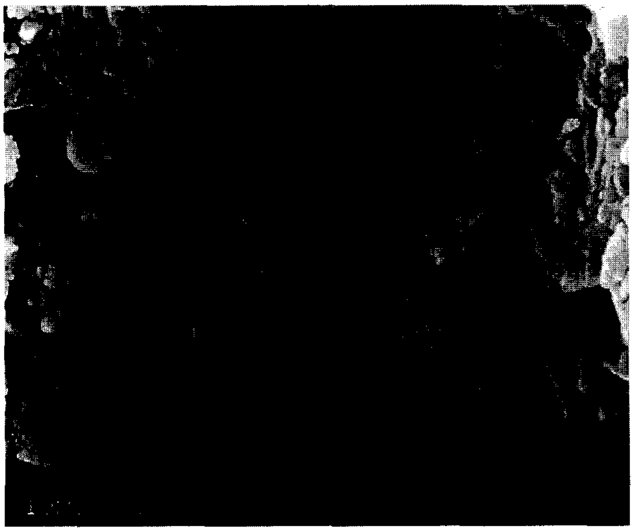

Fig. 11. SEM secondary electron micrographs of sample 4 sintered in PD2 at 1427°C. (Carbide agglomerates were found between SiC particles).

also be a newly formed secondary carbide by the reversible reactions inside the sample.

Samples sintered in PD3 were never well densified and weight losses were relatively large as shown in Fig. 6. Since PD3 was Si-rich (A_{Si} = 1), A_C in PD3 was the least. The total equilibrium partial pressure inside PD3 should be always lower than that inside the samples, where A_C is slightly less than stoichiometric (Fig. 3). Materials inside samples may be transferred to powder bed (PD3) by an expansion of the gases inside the samples. Even for samples 1 and 2 sintered in PD3, the sintering temperatures were relatively low, and the relative densities were lower than those sintered in PD1 and PD2. At higher sintering temperatures, above 1507°C, e.g. samples 5–8, the predominant reaction both inside the samples and inside PD3 is reaction (9) instead of reaction (1). The gas pressure by reaction (9) is higher than that by reaction (1) in the whole range of A_C (Fig. 1). Even though the equilibrium between PD3 and the samples may also be established and the A_C inside the samples may be also reduced to approach the minimum (A_{Si} = 1), and the total partial pressure inside the samples may be lower than that before the equilibrium, the absolute pressure is high, about 0·21 × 10^5 Pa, 3·82 × 10^5 Pa and 51·08 × 10^5 Pa for samples 6 (1527°C), 7 (1677°C) and 8 (1777°C), respectively according to Table 1. Silicon-rich powder beds (PD3) may never favour the sintering. XRD for sample 7 (PD3 1677°C) also gave Li_2C_2 (Fig. 7E) which indicated that reaction (9) may be predominant at 1677°C. Weight loss in Fig. 6 was not significantly larger than for other cases even though relative density was lower.

It becomes necessary to recall that the calculation results in Section 2 are all for equilibrium states; equilibrium between SiC and LAS (in either powder bed or in sample), and the equilibrium partial pressures of evaporating phases are, according to the calculations, very high, e.g. 77309.13 × 10^5 Pa for A_C = 1 at 1727°C (Fig. 3 and Table 1). It seems, therefore, that kinetic factors have to be considered in most cases. Jacobson *et al.*[9] studied the kinetics of the reaction of SiC with SiO_2 and showed that the reaction from commencement to equilibrium may need 2–3 h or longer. The sintering time of this study was only 30 min, which probably means that the results reported here were far away from equilibrium. Explanation of these results on the basis of thermodynamic calculations may be only referred to as the tendency of these reactions. Kinetic considerations are beyond the scope of this paper, but it is suggested that kinetic resistance could be used to avoid these reactions which are harmful to sintering. Lowering the temperature of sintering via adjusting compositions in LAS melts not only lowered equilibrium partial pressures but also offered a high kinetic resistance.

Another equilibrium discussed above is the equilibrium between powder bed and sample. A_C inside samples was initially almost the same (28·8 wt% of carbon in SiC, slightly less than stoichiometric). During the equilibration between powder bed and sample, the A_C inside the samples and the A_C in powder beds will approach each other. This equilibrium may also have kinetic resistance. In the sintering of samples 1 (PD2 1127°C) and 2 (PD2 1177°C), the kinetic resistance may be too high to increase A_C inside the samples to reach the equilibrium so that the reactions inside the samples were effectively inhibited and successful sintering was realised. During sintering at higher temperatures, the kinetic resistance towards equilibrium will be reduced and carbon-rich powder beds will not help with the densification of the samples.

5 Conclusions

1 Thermodynamics has predicted that SiC reacts with the components in LAS melts. The equilibrium partial pressures of SiO, CO and Al_2O have been calculated by varying carbon activity and equilibrium temperature.

2 SiC/40 v% LAS (65·2 wt% SiO_2, 15·0 wt% Al_2O_3, 19·8 wt% Li_2O or 55·0 wt% SiO_2, 22·5 wt% Al_2O_3, 22·5 wt% Li_2O) has been successfully sintered at low sintering temperatures (1127°C and 1177°C, respectively) by using a powder bed with unity carbon activity. High carbon activity in powder bed and low sintering temperature inhibited the reactions producing evaporating phases inside the samples.

3 SiC/40 v% LAS (other compositions) had to be sintered at higher temperatures and the sintering was less successful. This could be attributed to the reactions of SiC with the components of LAS. Thermodynamic explanation, XRD and SEM observations all suggested that these reactions were responsible for the unsuccessful sintering.

4 The reactions of SiC with LAS could be controlled by changing carbon activity both in the powder bed and in the samples and by lowering sintering temperature. Advantages in kinetic resistance should always be taken for good sintering.

Acknowledgement

The authors acknowledge Zhejiang University for permitting Dr Yi Pan a leave of absence for working in The Department of Ceramics and Glass Engineering, University of Aveiro, Portugal.

References

1. Alliegro, R. A., Coffin, L. B. & Tinklepaugh, J. R., Pressure sintered silicon carbide. *J. Am. Ceram. Soc.*, **39** (1956) 386–9.
2. Lange, F. F., Hot-pressing behaviour of silicon carbide powder with additions of aluminium oxide. *J. Mater. Sci.*, **10** (1975) 314–20.
3. Omori, M. & Takei, H., Preparation of pressureless sintered SiC-Y_2O_3-Al_2O_3. *J. Mater. Sci.*, **23** (1988) 3744–9.
4. Bocker, W. & Hausner, H., The influence of boron and carbon additions on the microstructure of sintered alpha silicon carbide. *Powder Metall. Int.*, **10** (1978) 87–90.
5. Liu Zhien, Sun Yihui, Du Xijiang & Cheng Jijian, Preparation and crystallisation of ultrafine Li_2O–Al_2O_3–SiO_2 powders. *J. Mater. Sci.*, **30** (1995) 390–4.
6. Panek, Z., Liquid phase sintering of chemically unstable silicon carbide-lithium magnesium aluminosilicate-titania composites, *J. Mater. Sci.*, **29** (1994) 5383–9.
7. Chase, M. W., Jr, Davies, C. A., Downey, J. R., Frurip D. J., McDonald, R. A. & Syverud, A. N. *JANAF Thermodynamic Tables* (3rd edn). American Chemical Society and American Institute of Physics for the National Bureau of Standards, New York, 1985.
8. Misra, A. K., Thermochemical analysis of the silicon carbide-alumina reaction with reference to liquid phase sintering of silicon carbide, *J. Am. Ceram. Soc.*, **74** (1991) 345–51.
9. Jacobson, N. S., Lee, K. N. & Fox, D. S., Reaction of silicon carbide (IV) oxide at elevated temperatures, *J. Am. Ceram. Soc.*, **75** (1992) 1603–11.
10. Levin, E. M., Robins, C. R. & McMurdie, H. F., *Phase Diagram for Ceramists. 1969 supplement*. America Ceramic Society, 1969.
11. Sacramento, J. M. G., Si_3N_4/SiC Composites Processed with Liquid Phases in LAS System. PhD Dissertation, University of Aveiro, 1993.
12. Almeida, J. C. M., Sacramento, J. M. G., Correia, R. N., Fonseca, A. T. & Baptista, J. L., Dispersion and packing of mixtures of Si_3N_4 powders with SiC whiskers. In *Fabrication Technology British Ceramic Proceedings* ed. R. W. Davidge & D. P.Thompson, 1989, pp. 179–86.
13. Kingery, W. D., Bowen H. K. & Uhlmann, D. R., *Introduction to Ceramics*. John Wiley & Sons, New York, 1975, pp. 491–501.
14. Miller, P. D., Lee, J. G. & Cutler, I. B., The reaction of silica with carbon and silicon carbide. *J. Am. Ceram. Soc.*, **62** (1979) 147–9.